Realistic three-nucleon effective interactions.

M. P. Kartamyshev, M. Hjorth-Jensen, T. Engeland, and E. Osnes

Department of Physics and Centre of Mathematics for Applications,

University of Oslo, N-0316 Oslo, Norway

(Dated: May 21, 2009)

Abstract

Importance of effective three-nucleon interactions in medium and heavy nuclei is still an open question. In this work we construct the effective three-nucleon interaction employing framework of the folded-diagram theory of Kuo and collaborators. To investigate influence of the effective three-nucleon interaction on nuclear spectra and binding energies, we perform shell-model calculations of selected *s*-*d* and *p*-*f* shell nuclei.

PACS numbers:

I. INTRODUCTION

II. THEORETICAL FRAMEWORK

Microscopic nuclear structure calculations aim to describe the properties of finite nuclei in terms of their constituent particles and the interactions among them. The corresponding many-body Schrödinger equation

$$H\Psi_i(1,...,A) = E_i\Psi_i(1,...,A) \tag{1}$$

is practically intractable in the full Hilbert space and one has to seek viable approximations to Eq. 1.

In the nuclear shell model calculations, one is normally only interested in solving Eq. 1 for certain low-lying eigen-states. One further assumes that these states of nuclei can described considering several valence nucleons that occupy space spanned by few physically selected orbitals, the so called model space. The full Hilbert space is then divided into a model space with an associated projection operator P and an excluded space defined by a projection operator $Q = 1 - P$. Eq. 1 can consequently be rewritten as a secular equation

$$PH_{\text{eff}}P\Psi_\mu = P(H_0 + R)P\Psi_\mu = E_\mu P\Psi_\mu \tag{2}$$

where H_{eff} is an effective hamiltonian acting solely within the chosen model space. $H_0 = T + U$ is the unperturbed Hamiltonian, with T denoting the kinetic energy and U is an auxilary potential. The effective interaction R for the system containing N nucleons in the model space can be written as

$$R = \sum_{i=1}^{N} R^{(i)} \tag{3}$$

with $R^{(1)}$, $R^{(2)}$, $R^{(3)}$, ... being one-body, two-body, three-body, etc components of the effective interaction.

In the nuclear shell model calculations it is customary to add the one-body effective interaction $R^{(1)}$ to the unperturbed part of the effective hamiltonian, so that

$$H_{\text{eff}} = \tilde{H}_0 + R^{(2)} + R^{(3)} + \dots \tag{4}$$

wher $\tilde{H}_0 = H_0 + R^{(1)}$. This allows one to replace the eigenvalues of $\tilde{H}_0$ by the empirical single-particle energies for the nucleon orbitals of our model space.

The remaining quantity to calculate is the effective interaction and our recipy for construction R is briefly reviewed below. The reader is refered to Ref. [2] for further details.

Our scheme to obtain R starts with a free nucleon-nucleon interaction V_{NN}, appropriate for nuclear physics at low and intermediate energies. Thereafter we need to handle the fact that the strong repulsive core of the nucleon-nucleon potential V_{NN} is unsuitable for perturbative approaches. This problem is dealt with by introducing the reaction matrix G, that renormalizes the strong repulsive short-range part of the NN interaction and is obtained by the solving the Bethe-Goldstone equation

$$G(\omega) = V_{NN} + V_{NN}\frac{Q_G}{\omega - H_0}G(\omega) \tag{5}$$

where ω is the unperturbed energy of the interacting nucleons. The operator Q_G, commonly referred to as the Pauli operator, is a projection operator that prevents the interacting nucleons from scattering into states occupied by other nucleons. Diagrammatically the G matrix is the sum over all particle ladder type diagrams. The physical interpretation is that the particles must interact with each other an infinite number of times to produce a finite interaction. In this work we solve the Bethe-Goldstone equation emploing the so-called double-partitioning scheme discussed, for example, in Ref. [2].

Having obtained the G matrix, the effective interaction R is constructed employing the folded-diagram theory [3, 4], formulated for the case of degenerate model space. One starts with introduction of the so-called $\widehat{Q}$-box, defined as

$$\widehat{Q}(\epsilon) = PH_1P + PH_1Q\frac{1}{\epsilon - QHQ}QH_1P \tag{6}$$

with $H_1 = G - U$ and ϵ is the unperturbed energy of the (degenerate) model space states, i.e $PH_0P = \epsilon P$. Diagrammatically the $\widehat{Q}$-box is an infinite sum of irreducible and valence-linked diagrams. A diagram is said to be irreducible if between each pair of vertices there is at least one single particle state which belongs to the excluded space Q. In a valence-linked diagram all interactions are linked (via fermion lines) to at least one valence (or model space) line. A valence-linked diagram can be either connected (consisting of a single piece) or disconnected. In the final expression for the effective interaction, including folded diagrams as well, the disconnected diagrams are found to cancel out [3, 4].

The R is then obtained summing the folded diagrams series

$$R = \widehat{Q} - \widehat{Q}'\int\widehat{Q} + \widehat{Q}'\int\widehat{Q}\int\widehat{Q} - \widehat{Q}'\int\widehat{Q}\int\widehat{Q}\int\widehat{Q} + \ldots \tag{7}$$

The integral sign in Eq. 7 represents the generalized folding operation and $\widehat{Q}'$ is obtained from $\widehat{Q}$ by removing all terms which are first order in the nucleon-nucleon potential V_{NN}. Note that Eq. 7 is general and valid also when energies of model space states are not all degenerate.

Assuming that the model space is degenerate, the folded diagram expansion in Eq. 7 can be summed to all orders by means of the Lee-Suzuki iterative scheme [5], where effective interaction at the n-th iteration is given by

$$R^{(n)} = \left(1 - Q_1 - \sum_{m=2}^{n-1} \widehat{Q}_m \prod_{k=n-m+1}^{n-1} R^{(k)}\right)^{-1} \widehat{Q} \qquad \text{with} \qquad \widehat{Q}_m = \frac{1}{m!}\frac{d^m \widehat{Q}(\epsilon_0)}{d\epsilon^m} \tag{8}$$

The first iteration $R^{(1)}$ is represented by just the $\widehat{Q}$-box and ϵ_0 is value the unperturbed energy of particles in the model space.

Having constructed the effective interaction R we proceed with the shell model calculations, finding solutions to Eq. 2 by means of the Lanczo's algorithm. The technique is described in detail in Ref. [9] and implemented via the Oslo Shell Model code [10].

III. THREE-BODY EFFECTIVE INTERACTION

As pointed out in the previous section, to construct effective interaction for systems with N nucleons in the model space, one in principle needs to construct one-, two-, and up to N-body components of the effective interaction R. In the actual shell model calculations it is, however, customary to consider only one- and two-body components of the effective interaction, $R^{(1)}$ and $R^{(2)}$. The purpose of this work is to investigate importance of the three-body component of effective interaction, $R^{(3)}$.

We solve Eq. 7 in basis formed by three-nucleon M-scheme states, thus obtaining three-body effective interaction R containing contributions from both one-, two- and three-body components. These components need to be disentangled from the complete R in order to proceed with the shell model calculations. This issue has already been addressed in [11] and in this section we briefly repeat the discussion therein,

Consider situation where the model space contains one nucleon, i.e. $N = 1$. In this case the $\widehat{Q}$-box will contain only one-body connected diagrams, having form schematically displayed on Fig. 1. We will later refer to these diagrams as belonging to the class $S^{(\sigma)}$. Solving Eq. 8 for this case yields one-body effective interaction, $R^{(1)}$.

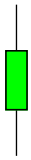

FIG. 1: Schematic picture of diagrams entering the one-body $\widehat{Q}$-box.

Now consider the case of two nucleons in the model space, $N = 2$. The $\widehat{Q}$-box will now contain both one- and two-body diagrams, schematically shown on Fig. 2. Classes $D^{(\sigma)}$ and $D^{(\delta)}$ contain all two-body connected diagrams, while class $D^{(\sigma\sigma)}$ contains two-body disconnected diagrams. Diagrams from all these classes have to be included in the two-body $\widehat{Q}$-box to generate all possible two-body folded diagrams, contributing to the resulting two-body effective interaction R.

The result for two-body R obtained solving Eq. 8 will now contain contributions from both the one-body component $R^{(1)}$, and the two-body component $R^{(2)}$. The one-body component $R^{(1)}$ is already determined, this is just the one-body effective interaction constructed

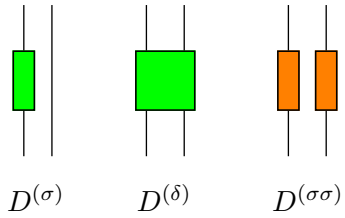

FIG. 2: Classes of diagrams entering the two-body $\widehat{Q}$-box.

previously. Thus the two-body component $R^{(2)}$ can be extracted from the resulting R making use of

$$\langle ab|\, R\, |cd\rangle = \langle ab|\, R^{(2)}\, |cd\rangle + \left(\langle a|\, R^{(1)}\, |a\rangle + \langle b|\, R^{(1)}\, |b\rangle\right) \delta_{ac}\, \delta_{bd} \tag{9}$$

We assume that the initial and final model space single-particle states in Fig. 2 are ordered so that $a < b$, $c < d$. The two-body M-scheme matrix elements are "antisymmetrized", i.e. $\langle ab|\, V\, |cd\rangle$ implies $\langle ab|\, V\, |cd - dc\rangle$.

Let us now turn attention to the case of three nucleons in the model space, $N = 3$. Classes of diagrams entering the three-body $\widehat{Q}$-box are schematically sketched on Fig. 3. Diagrams entering $T^{(\sigma)}, T^{(\delta)}$ and $T^{(\sigma\sigma)}$ classes are three-body generalizations of two-body diagrams belonging to classes $D^{(\sigma)}, D^{(\delta)}$ and $D^{(\sigma\sigma)}$ correspondingly. There are also new classes of diagrams, as compared to the two-body case. Class $T^{(\tau)}$ contains connected three-body diagrams, which connect together three valence lines. Classes $T^{(\sigma\sigma\sigma)}$ and $T^{(\delta\sigma)}$ are contain disconnected diagrams, which first appear only for $N = 3$. The resulting three-body effective

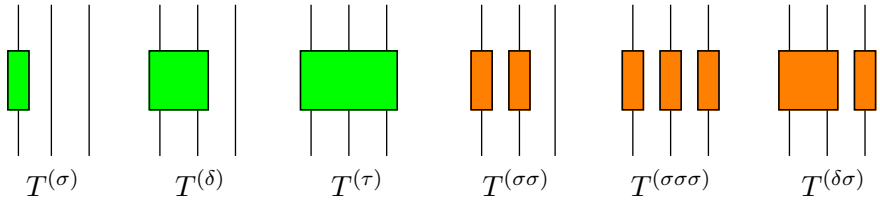

FIG. 3: Classes of diagrams entering the three-body $\widehat{Q}$-box.

interaction R will now contain contribution from the three-body component $R^{(3)}$, where all three valence lines are connected together, contributions from the two-body component $R^{(2)}$, acting on all possible pairs of lines, as well as contributions from the one-body component $R^{(1)}$, acting on each line separately. Using Eq. 9, the three-body component of the effective

interaction, $V^{(3)}$, can be disentangled from the solution of Eq. 8 as

$$\begin{aligned}
\langle ijk|\, R\, |lmn\rangle &= \langle ijk|\, R^{(3)}\, |lmn\rangle + \\
&\langle ij|\, R^{(2)}\, |lm\rangle\ \delta_{kn} - \langle ij|\, R^{(2)}\, |ln\rangle\ \delta_{km} - \langle ij|\, R^{(2)}\, |nm\rangle\ \delta_{kl} - \\
&\langle ik|\, R^{(2)}\, |lm\rangle\ \delta_{jn} + \langle ik|\, R^{(2)}\, |ln\rangle\ \delta_{jm} + \langle ik|\, R^{(2)}\, |nm\rangle\ \delta_{jl} - \\
&\langle kj|\, R^{(2)}\, |lm\rangle\ \delta_{in} + \langle kj|\, R^{(2)}\, |ln\rangle\ \delta_{im} + \langle kj|\, R^{(2)}\, |nm\rangle\ \delta_{il} + \\
&\left(\langle i|\, R^{(1)}\, |l\rangle + \langle j|\, R^{(1)}\, |m\rangle + \langle k|\, R^{(1)}\, |n\rangle\right) \delta_{il}\, \delta_{jm}\, \delta_{kn}
\end{aligned} \tag{10}$$

For a given matrix element only a few of the delta functions of Eq. 11 will be nonzero. Since the inital and final states are in a chosen standard order the one-body component $R^{(1)}$ only contributes when $i = l$, $j = m$ and $k = n$. The M-scheme three-body matrix elements are "antisymmetrized", i.e $\langle ijk|\, R\, |lmn\rangle$ implies $\langle ijk|\, R\, |ijk - ikj + kij - jik + jki - kji\rangle$, labelling in order for particle numbers 1, 2 and 3.

A. Diagrammatic content of the three-body $\widehat{Q}$-box

Having outlined the scheme to separate one-, two- and three-body components of the effective interaction from the solution of Eq. 8 for the three-nucleon system, it remains to specify diagrammatic content of the three-body $\widehat{Q}$-box. Ideally, the $\widehat{Q}$-box should contain irreducible and valence linked diagrams up to all orders. However, it is not practically possible to compute all $\widehat{Q}$-box diagrams, and in the actual calculations two approximations are typically introduced.

The first approximation addresses connected $\widehat{Q}$-box diagrams, that are customarily computed to the third order at most. Challenge of accounting for fourth and higher order diagrams lies in large amount of such diagrams. One could resort to automatic computation of Goldstone diagrams [12] in order to cope with this difficulty. This, however, is not a subject of the present work.

The second approximation is related to the disconnected $\widehat{Q}$-box diagrams. As previously mentioned, all disconnected diagrams entering Eq. 7 cancel out among them. This means that if one could compute the $\widehat{Q}$-box exactly, the final result for the R would contain contributions from connected diagrams only, both folded and non-folded. In the actual calculations, however, one always operates with $\widehat{Q}$-box having truncated diagrammatic content, viz. the first approximation. The effective interaction obtained starting from a $\widehat{Q}$-box

containing only a limited set of relevant diagrams will always contain contributions from disconnected diagrams. This is because cancellation of disconnected contributions to R involves disconnected diagrams from different folds, yet with the same amount of interaction vertices.

Computing the two-body effective interaction, the common practice is to neglect contributions from the two-body disconnected diagrams $D^{(\sigma\sigma)}$ completely. This approximation greately simplifies calculation of the two-body $\widehat{Q}$-box and is justified by the fact that values of disconnected two-body diagrams are small. Taking $D^{(\sigma\sigma)}$ into account introduces only a small change to the matrix elements of two-body component of the effective interaction, $R^{(2)}$.

Contrary to the two-body case, small disconnected diagrams may play a non-negligible role for the three-body effective interaction, as the three-body component of effective interaction, $R^{(3)}$, is also a small contribution. In this work we attempt to investigate importance of the disconnected $\widehat{Q}$-box terms for the three-body effective interaction.

Calculation of the disconnected terms employing diagram rules is a heavy computational task because of the large amount of higher order diagrams that needs to be considered. It is, however, possible to establish a scheme that allows to partially account for contributions of disconnected $\widehat{Q}$-box diagrams making use of their cancellation properties. In what follows we briefly demonstrate the underlying idea considering disconnected contributions to the two-body component of the effective interaction, $R^{(2)}$.

The disconnected contributions to $R^{(2)}$ arise due to the disconnected non-folded diagrams entering class $D^{(\sigma\sigma)}$ of Fig. 2, as well as disconnected folded diagrams. To account for both of the above contributions one only needs to compute the $D^{(\sigma\sigma)}$ term. Having constructed the $\widehat{Q}$-box, one will generate the folded disconnected contributions during iteration procedure defined by Eq. 8. Cancellation of disconnected diagrams implies that $D^{(\sigma\sigma)}$ diagrams are cancelled out by the corresponding disconnected diagrams from the first fold, as schematically depicted on Fig. 4.

The first fold diagrams of Fig. 4 are obtained by folding $D^{(\sigma)}$ term on itself. The $D^{(\sigma)}$ diagrams are the two-body generalization of one-body connected diagrams, i.e.

$$\langle ab|\, D^{(\sigma)}\, |cd\rangle = \langle a|\, S^{(\sigma)}\, |c\rangle\, \delta_{bd} + \langle b|\, S^{(\sigma)}\, |d\rangle\, \delta_{ac} \tag{11}$$

Writing down algebraic equivalents for diagrams of Fig. 4, for the $D^{(\sigma\sigma)}$ term one readily

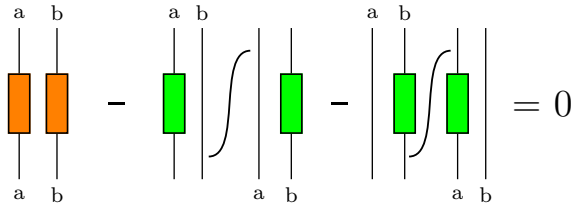

FIG. 4: One of the sets of two-body disconnected diagrams which cancel out in the folding procedure.

obtains

$$\langle ab|\, D^{(\sigma\sigma)}\, |cd\rangle = -\Big[\frac{d\left(\langle a|\, S^{(\sigma)}\, |a\rangle\, \langle b|\, S^{(\sigma)}\, |b\rangle\right)}{d\epsilon}\Big]_{\epsilon=\epsilon_0} \tag{12}$$

where we have used the general expression for an n-folded diagram [4].

$$\widehat{Q}' \int \widehat{Q} \int \widehat{Q} \int \ldots \int \widehat{Q} = \Bigg[\sum_{m_1,m_2,\ldots,m_n} \frac{1}{m_1!} \frac{d_1^m \widehat{Q}'}{d\epsilon^{m_1}} \; \frac{1}{m_2!} \frac{d_2^m \widehat{Q}}{d\epsilon^{m_2}} \; \ldots \; \frac{1}{m_n!} \frac{d_n^m \widehat{Q}}{d\epsilon^{m_n}} \; \widehat{Q} \Bigg]_{\epsilon=\epsilon_0} \tag{13}$$

The result of Eq. 12 suggests that it suffices to compute diagrams of $D^{(\sigma)}$ term and employ cancellation properties of disconnected diagrams to obtain values of diagrams entering $D^{(\sigma\sigma)}$ term as a whole, without computing diagrams entering $D^{(\sigma\sigma)}$ individually. As we cannot compute all $D^{(\sigma)}$ diagrams, the $D^{(\sigma\sigma)}$ constructed this way will contain only a sub-class of all possible two-body non-folded disconnected diagrams. Yet, one insures that disconnected diagrams of Fig. 4 will not be contribute to the effective interaction if $D^{(\sigma\sigma)}$ is constructed according to Eq. 12.

The above ideas can be extended to computation of starting energy derivatives of $D^{(\sigma\sigma)}$ diagrams, needed for construction of the effective interaction employing Eq. 8. It is, however, not possible to achieve exact cancellation of disconnected terms that depend on derivatives of $D^{(\sigma\sigma)}$ diagrams, unless $D^{(\sigma)}$ diagrams are computed to all orders.

Effective interaction obtained starting from $\widehat{Q}$-box containing a limited set of diagrams will always contain contributions from disconnected diagrams. In our calculations we attempt to minimize such contributions to the three-body effective interaction and include disconnected diagrams in both two-body and three-body $\widehat{Q}$-boxes. At the present stage we omit contribitons from the derivatives of disconnected $\widehat{Q}$-box terms, except for the first derivative of $D^{(\sigma\sigma)}$, needed for approximation of $T^{(\sigma\sigma\sigma)}$ term. Further details and expressions for the disconnected terms used in the present work are given in the Appendix.

IV. RESULTS AND DISSCUSSION

We apply the formalism presented in previous section to construction of the effective interaction for the ^{16}O isotopes. As the two-nucleon iteraction we use is the G-matrix obtained using N3LO potential as the 'bare' NN interaction. The G-matrix elements are computed in harmonic oscillator basis with $\hbar\omega = 14$ MeV.

The connected one-body and two-body diagrams are evaluated up to third order: for the comlete listing of these diagrams the reader is referred to Appendix A.2 of [2]. The three-body connected diagrams entering class $T^{(\tau)}$ of Fig. 3 are included up to second order, and are displayed on Fig. 5.

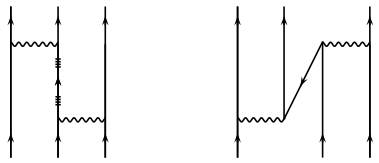

FIG. 5: Three-body connected diagrams included in the three-body $\widehat{Q}$-box.

The starting energy derivatives of the connected $\widehat{Q}$-box diagrams are included up to 13th order and computed with machine precision using automatic differentiation package of [13].

The iterative scheme given by Eq. 8 converges rather quickly, and typically 20 iterations are sufficient to obtain stable solution for the three-body effective interaction.

V. CONCLUSIONS

APPENDIX A: DISCONNECTED DIAGRAMS OF THE THREE-BODY $\widehat{Q}$-BOX

It can be shown [4] that all disconnected diagrams (folded and non-folded) cancel out in the folding process, so that the effective interaction contains contributions from connected diagrams only. More precisely, the disconnected diagrams from different folds and with the same amount of interaction vertices cancel out exactly. This cancellation property can be used for evaluation of the disconnected $\widehat{Q}$-box terms.

Let us start with the two-body disconnected diagrams belonging to class $D^{(\sigma\sigma)}$, Fig. 2. The two-body non-folded diagrams are cancelled out by disconnected folded diagrams from the first fold, as shown on Fig. 4. Introduce shorthand notations

$$O_{a,c} \equiv \langle a|\, O\, |c\rangle \qquad O_{ab,cd} \equiv \langle ab|\, O\, |cd\rangle \qquad O_{ijk,lmn} \equiv \langle ijk|\, O\, |lmn\rangle \tag{A1}$$

algebraic equivalent for diagrams on Fig. 4 reads

$$D^{(\sigma\sigma)}_{ab,ab} - S_{a,a}\int S_{b,b} - dS_{b,b}\int S_{a,a} = D^{(\sigma\sigma)}_{ab,ab} + \frac{dS_{a,a}}{d\omega}S_{b,b} + \frac{dS_{b,b}}{d\omega}S_{a,a} = 0 \tag{A2}$$

where we have used $A\int B = \frac{dA}{d\omega}B$ for the once folded diagrams [3, 4]. For the diagrams belonging to $D^{(\sigma\sigma)}$ class we get

$$D^{(\sigma\sigma)}_{ab,ab} = -\frac{d}{d\omega}\Big[\, S_{a,a}\, S_{b,b}\Big] \tag{A3}$$

Class $T^{(\sigma\sigma)}$ contain all possible topologically distinct three-body contributions from two-body diagrams belonging to class $D^{(\sigma\sigma)}$. Hence the expression for $T^{(\sigma\sigma)}$ class diagrams reads

$$\langle ijk|\, T^{(\sigma\sigma)}\, |lmn\rangle = -\frac{d}{d\omega}(S_{i,j}S_{j,m} + S_{i,j}S_{k,n} + S_{j,m}S_{k,n})\,\delta_{ij}\,\delta_{jm}\,\delta_{kn} \tag{A4}$$

$T^{(\delta\sigma)}$ is displayed on Fig. 6

Taking into account all possible topologically distinct diagrams, for the $T^{(\delta\sigma)}$ contribution we get

$$\begin{aligned}\langle ijk|\, T^{(\delta\sigma)}\, |lmn\rangle = -\frac{d}{d\omega}\Big[& D^{(\delta)}_{ij,lm}\, S_{k,n} \;-\; D^{(\delta)}_{ij,ln}\, S_{k,m} - D^{(\delta)}_{ij,nm}\, S_{k,l} - \\ & D^{(\delta)}_{ik,lm}\, S_{j,n} \;+\; D^{(\delta)}_{ik,ln}\, S_{j,m} + D^{(\delta)}_{ik,nm}\, S_{j,l} - \\ & D^{(\delta)}_{kj,lm}\, S_{i,n} \;+\; D^{(\delta)}_{kj,ln}\, S_{i,m} + D^{(\delta)}_{kj,nm}\, S_{i,l}\Big]\end{aligned} \tag{A5}$$

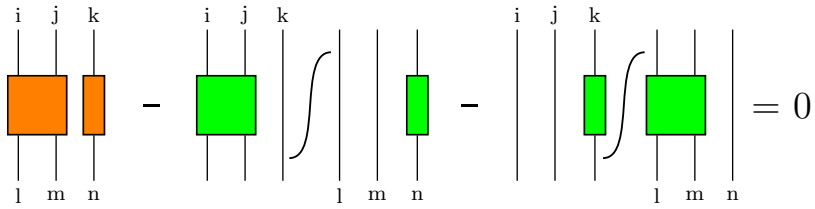

FIG. 6: Set of three-body disconnected diagrams which cancel out among themselves.

Diagrams from class $T^{(\sigma\sigma\sigma)}$ are composed of three disconnected branches. Cancelling contributions will therefore come from diagrams belonging to both first and second fold, as shown on Fig. 7

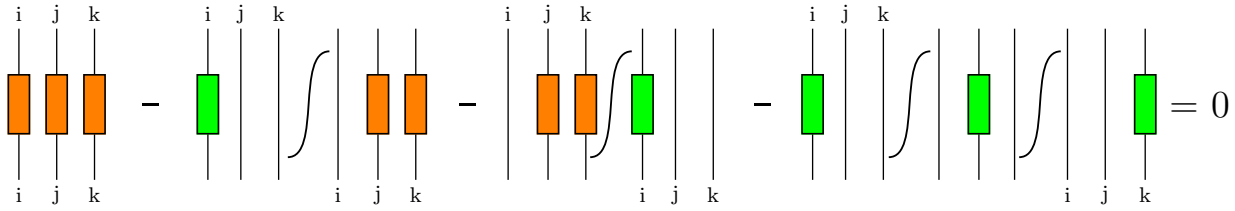

FIG. 7: Set of three-body disconnected diagrams which cancel out among themselves.

For the twice folded diagram one gets [4]:

$$\widehat{A}\int\widehat{B}\int\widehat{C} = \left[\frac{1}{2}\frac{d^2\widehat{A}}{d\omega^2}\widehat{B}\widehat{C} + \frac{d\widehat{A}}{d\omega}\frac{d\widehat{B}}{d\omega}\widehat{C}\right]_{\omega_0} \tag{A6}$$

Using result for the diagrams of class $T^{(\sigma\sigma)}$ (A5), expression for the disconnected diagrams belonging to the class $T^{(\sigma\sigma\sigma)}$ can be cast in the following form:

$$\begin{aligned}\langle ijk|\,T^{(\sigma\sigma\sigma)}\,|lmn\rangle = \frac{1}{2}\left[\frac{d^2I}{d\omega^2}(J+K)^2 + \frac{d^2J}{d\omega^2}(I+K)^2 + \frac{d^2J}{d\omega^2}(I+J)^2\right]\delta_{il}\,\delta_{il}\,\delta_{il} + \\ \left[\frac{dI}{d\omega}\frac{dJ}{d\omega}(I+J+2K) + \frac{dI}{d\omega}\frac{dK}{d\omega}(I+K+2J) + \frac{dJ}{d\omega}\frac{dK}{d\omega}(J+K+2I)\right]\delta_{il}\,\delta_{il}\,\delta_{il}\end{aligned} \tag{A7}$$

where we have used $I = S_{i,i}$, $J = S_{j,j}$, $K = S_{k,k}$.

---

[1] R. B. Wiringa and S. C. Pieper, Phys. Rev. Lett. **89**, 182501, (2002).

[2] M. Hjorth-Jensen, T. T. S. Kuo and E. Osnes, Phys. Rep. **261**, 125 (1995).

[3] T. T. S. Kuo, S. Y. Lee, and K. F. Ratcliff, Nucl. Phys. A**176**, 65 (1971).

[4] T. T. S. Kuo and E. Osnes, Folded-Diagram Theory of the Effective Interaction in Atomic Nuclei, Springer Lecture Noters in Physics (Springer, Berlin, 1990) Vol. 364

[5] S. Y. Lee and K. Suzuki, Phys. Lett. B **91** 79 (1980), K. Suzuki and S. Y. Lee, Prog. Theor. Phys. **64** 2091 (1980).

[6] R. Machleidt, F. Sammarruca and Y. Song, Phys. Rev. C **53**, R1483 (1996).

[7] R. Machleidt, Adv. Nucl. Phys. **19**, 189 (1989).

[8] See http://folk.uio.no/mhjensen/CENS for codes and shell model interactions for various closed shell cores.

[9] R. R. Whitehead, A. Watt, B. J. Cole, and I. Morrison, Adv. Nucl. Phys. **9**, 123 (1977)

[10] T. Engeland, the Oslo shell model code, 1991-2006, unpublished. See also Ref. [8] for further information.

[11] P. J. Ellis, T. Engeland, M. Hjorth-Jensen, M. P. Kartamyshev, E. Osnes, Phys. Rev. C**71**, 034301, (2005)

[12] B. D. Chang, C. M. Vincent, S. S. M. Wong Phys. Rev. C **30**, 1055-1062, (1984)

[13] G. M. von Hippel Comput. Phys. Comm. **176**, 710-711, (2007)